Effect of N-Terminal Truncation and Solution Conditions on Chemokine Dimer Stability: Nuclear Magnetic Resonance Structural Analysis of Macrophage Inflammatory Protein 1β Mutants[†]

Jennifer S. Laurence,[‡] Andy C. LiWang,[§] and Patricia J. LiWang*[,‡]

Department of Chemistry and Department of Medicinal Chemistry and Medical Pharmacology, Purdue University, West Lafayette, Indiana 47907-1393

Received February 10, 1998; Revised Manuscript Received April 24, 1998

ABSTRACT: Chemokines (chemotactic cytokines) are a family of immune system proteins, several of which have been shown to block human immunodeficiency virus (HIV) infection in various cell types. While the solved structures of most chemokines reveal protein dimers, evidence has accumulated for the biological activity of individual chemokine monomers, and a debate has arisen regarding the biological role of the chemokine dimer. Concurrent with this debate, several N-terminal truncations and modifications in the CC subfamily of chemokines have been shown to have functional significance, in many cases antagonizing their respective receptors and in some cases retaining the ability to block HIV entry to the cell. As the dimer interface of CC chemokines is located at their N-terminus, a structural study of N-terminally truncated chemokines will address the effect that this type of mutation has on the dimer−monomer equilibrium. We have studied the structural consequences of N-terminal truncation in macrophage inflammatory protein 1β (MIP-1β), a CC chemokine that has been shown to block HIV infection. Examination of nuclear magnetic resonance (NMR) spectra of a series of N-terminally truncated MIP-1β variants reveals that these proteins possess a range of ability to dimerize. A mutant beginning at amino acid Asp6 [termed MIP(6)] has near wild-type dimer properties, while further truncation results in weakened dimer affinity. The mutant MIP(9) (beginning with amino acid Thr9) has been found to exist solely as a folded monomer. Relaxation measurements yield a rotational correlation time of 8.6 $\pm$ 0.1 ns for wild-type MIP-1β and 4.5 $\pm$ 0.1 ns for the MIP(9) mutant, consistent with a wild-type dimer and a fully monomeric MIP(9) variant. The presence of physiological salt concentration drastically changes the monomer−dimer equilibrium for both wild-type and most mutant proteins, heavily favoring the dimeric form of the protein. These results have implications for structure−function analysis of existing chemokine mutants as well as for the larger debate regarding the biological existence and activity of the chemokine dimer.

Human MIP-1β[1] is a member of the chemokine (chemotactic cytokine) family, a group of proteins that is active in the immune response, being involved in the recruitment and activation of lymphocytes and phagocytes to infected areas of the body (*1*, *2*). The chemokine family is broken down into two main subfamilies: members of the CC subfamily (so named because the N-terminal conserved cysteines are contiguous) include MIP-1β, MIP-1α, MCP-1, and RANTES. The CXC subfamily (named because members of this subfamily have an amino acid inserted between the conserved N-terminal cysteines) includes such molecules as IL-8, PF-4, and MGSA. Most three-dimensional structures that have been determined for wild-type proteins of both subfamilies reveal a multimeric protein, the most commonly described form being the dimer (*3*−*13*). Figure 1 shows a ribbon diagram of the structure of MIP-1β, the first CC chemokine structure reported (*3*). The protein has an N-terminal dimer interface with significant contact between the two monomers beginning at residue Gly4. With one possible exception (*7*), other CC chemokine structures have a similar dimer structure (*6*, *8*−*10*, *12*).

Three CC chemokines, MIP-1β, MIP-1α, and RANTES, have been shown to be able to block infection of macrophages by HIV-1 (*14*−*16*). This latter observation is due to the requirement of HIV for certain chemokine receptors in order to gain entry to a cell. If access to the chemokine receptor is blocked, productive infection does not occur. MIP-1β, MIP-1α, and RANTES have each been shown to be able to bind the CCR5 receptor, blocking access to HIV and protecting the cell from infection (*14*−*17*).

After their identification as important anti-HIV molecules, chemokines have come under intense scrutiny. Mutational work has revealed important areas for protein function but

[†] Funding was provided by the American Heart Association, Indiana Affiliate, Grant INN-96-BGIAO-228, and by the National Science Foundation, Research Planning Grant MCB-9797270.

* To whom correspondence should be addressed.

[‡] Department of Chemistry.

[§] Department of Medicinal Chemistry and Medical Pharmacology.

[1] Abbreviations: MIP-1β, macrophage inflammatory protein 1β; MIP-1α, macrophage inflammatory protein 1α; MCP, monocyte chemoattractant protein; RANTES, regulated on activation of normal T cell expressed and secreted; IL-8, interleukin-8; MGSA, melanoma growth-stimulatory activity; NAP-2, neutrophil-activating peptide 2; PF-4, platelet factor-4; NMR, nuclear magnetic resonance; HIV-1, human immunodeficiency virus type 1; HSQC, heteronuclear single quantum coherence; DSS, 2,2-dimethyl-2-silapentane-5-sulfonate, sodium salt; EDTA, ethylenediaminetetraacetic acid.

S0006-2960(98)00329-8 CCC: $15.00
Published on Web 06/11/1998

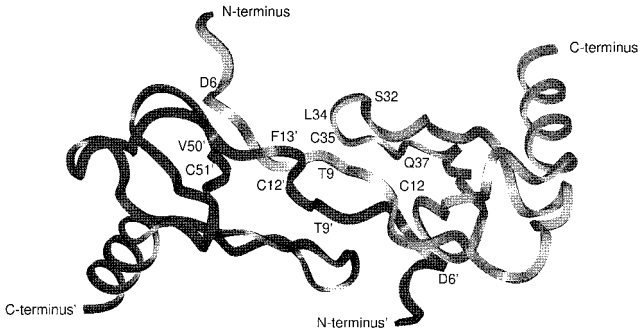

FIGURE 1: Ribbon diagram of the MIP-1β homodimer (*3*). Residues important for dimerization are labeled with their one-letter code followed by the number that corresponds to their position in the sequence. The second subunit is denoted by tic marks.

has not as yet provided a complete picture of their action. In particular, controversy has arisen over the form of the chemokine that productively binds its receptor. Despite the preponderance of chemokine multimers upon structure determination, structural studies do require high concentrations of protein. At presumed physiological concentrations these proteins are present in much lower amounts and may be predominantly monomeric (*18*−*21*).

Probably the largest body of work to date regarding the multimeric state of the active chemokine has been carried out on the CXC chemokine IL-8. In widely noted work, IL-8 was chemically synthesized to contain a methyl group on the amide nitrogen of Leu25, an important dimer interface residue (*18*). With the bulky methyl group unable to contribute to the H-bonding scheme of the β sheet in the dimer interface, this IL-8 variant was shown to be a monomer. This protein was still able to activate neutrophils, indicating that monomeric IL-8 is a functional chemokine (*18*). In later work, analytical ultracentrifugation was used to provide data that the apparent dimer equilibrium constant for wild-type IL-8, at 18 μM, is several orders of magnitude above the (presumably nanomolar) physiological concentrations of the protein (*19*). This suggested that, biologically, the monomeric form of IL-8 predominates.

Perhaps surprisingly, rather than settling the question of the importance of the CXC chemokine dimer, this work has led to more research addressing the question of whether *both* the dimer and the monomer form of the chemokine might be active. One group has multiply mutated IL-8 to produce a monomeric protein that is reduced in activity compared to the wild-type protein by only severalfold in a variety of assays (*22*). Yet the same group showed that cysteine cross-linked obligate IL-8 dimers also yielded near wild-type activity, although a wild-type monomer joined to a mutant monomer was also active (*23*). These workers also report that the dimer dissociation constant for wild-type IL-8 is dependent upon solution conditions (*22*). So while it appears that a monomeric IL-8 is certainly functional biologically, the dimer is also functional and may be present *in vivo* depending on local conditions.

Fewer direct studies have been carried out on the monomer versus dimer question with CC chemokines, and little is known about the structure of mutants from this subfamily. Reported dimer dissociation constants range from 35 μM for RANTES (*6*) and 33 μM for MCP-1 (*20*) to 40 nM for MIP-1β. [The value for MIP-1β remains a personal communication (P. Wingfield); in our laboratory we are currently working toward confirming this dissociation constant.] Some workers report that these values are dependent upon solution conditions (*3*, *6*), again raising the possibility that given the variety of cells and receptors contacted by these proteins, local environments may be manipulated to favor a specific multimeric state. Indeed, chemokines are able to bind heparin at the cell surface (*24*−*26*), suggesting that this may be a method of collecting and presenting chemokines to receptors at concentrations different than those circulating in the blood. Recent work has confirmed this, showing that glycosaminoglycans do act to significantly increase local concentrations of chemokines (*27*). Furthermore, cells treated to remove glycosaminoglycans showed decreased receptor binding by chemokines, revealing a concentration dependence that is consistent with chemokine multimers as active species (*27*).

In work with MCP-1, while the dimer dissociation constant for this CC chemokine has been reported to be much higher than presumed physiological concentrations (*20*), the presence of clearly detectable MCP-1 dimers at concentrations of 2 nM has been demonstrated, and covalently cross-linked MCP-1 dimers have been shown to be fully active (*28*).

Mutational work of chemokines has been carried out by several groups, with most studies focusing on the N-terminal region, as it has become apparent for both subfamilies that this region is critical for function (*29*−*33*). The results of these studies for CC chemokines have demonstrated the importance of residues at the N-terminus in both binding and activating chemokine receptors (*29*, *31*, *33*). This work in turn has led to interest in the use of modified chemokines as therapeutic agents (or as models of therapeutic agents) for the treatment of immune and inflammation-related disorders including AIDS (*31*, *34*).

While the N-terminus of CC chemokines is clearly crucial for receptor activation and may also play a role in receptor binding and specificity, the various data on chemokine mutants do not lead to a clear structural picture of chemokine action. If the CC chemokine monomer is indeed the only relevant biological form, then few data exist as a starting point to indicate the structure of a nondimerized CC chemokine, particularly at the crucial N-terminus. With few exceptions (*7*, *12*) the determined structures of CC chemokines reveal dimers, with the N-terminus involved in the oligomeric interface. If, on the other hand, the CC chemokine dimer plays a role in the biological activity of these proteins, then it is likely that the reason the N-terminal modifications significantly impact the function is because they disrupt the CC chemokine dimer interface.

We have undertaken a structural study of various N-terminal truncation mutants of the CC chemokine MIP-1β. This chemokine is unique in that is has been shown to directly block HIV infection and yet it activates only the CCR5 receptor, showing no activity against the several other characterized chemokine receptors (*17*). Therefore, modification of MIP-1β holds promise for yielding anti-HIV activity with minimal impact on other chemokine functions. Our results directly show the impact of N-terminal truncation on dimer stability and provide the first structural framework for interpretation of the effect of N-terminal changes to CC chemokines.

MATERIALS AND METHODS

Production and Purification of MIP-1β. Wild-type MIP-1β (cDNA kindly provided by W. Leonard) and MIP-1β mutants MIP(6) and MIP(9) were expressed in Novagen (Milwaukee, WI) pET32LIC expression vectors, which allow production of the desired protein along with a thioredoxin fusion tag. Vector construction for pET32LIC constructs was accomplished by using standard thermocycling polymerase reactions, with oligonucleotides as described in Novagen literature, to amplify the MIP-1β DNA. The amplified DNA was placed into the pET32LIC vector as instructed by the manufacturer and then sequenced. For each protein, the appropriate vector was transformed into BL21-(DE3) and an individual colony was subsequently grown in 1 L of minimal medium containing $^{15}NH_4Cl$ (Isotec, Miamisburg, OH) as the only nitrogen source. Cells were induced at $A_{550} = 0.9$ by adding IPTG (Calbiochem, La Jolla, CA) to 1 mM, and the cells were harvested by centrifugation after about 7 h. The cell pellet was resuspended in 500 mM NaCl, 20 mM Tris, pH 8, 1 mM EDTA, 5 mM benzamidine, and 5 mM β-mercaptoethanol, passed through a French press two times at 16 000 psi, and then centrifuged at 19000*g* for 1 h. The resulting pellet was then resuspended in 15 mL of 5 M guanidine hydrochloride, 50 mM NaCl, 20 mM Tris, pH 8, 1 mM EDTA, and 5 mM β-mercaptoethanol (overall buffer adjusted to pH 8). The resuspended protein was centrifuged at 15 000*g* for 30 min to remove insoluble material and subjected to refolding (*35*). The refolded protein solution was loaded onto a Ni chelating column (Pharmacia, Piscataway, NJ) and eluted with imidazole. The resulting purified thioredoxin−MIP-1β fusion protein was then diluted to about 0.5 mg/mL with 50 mM NaCl and 20 mM sodium phosphate, pH 7.2, and dialyzed against this buffer. Cleavage of the thioredoxin fusion tag was carried out with recombinant enterokinase (Novagen) and the cleaved protein was purified by C4 reversed-phase chromatography, using a Vydac column (Hesperia, CA) and the Biologic system (Bio-Rad Hercules, CA). The MIP(7) mutant was expressed in both pET32LIC and PET21d expression vectors (Novagen). The pET21dMIP(7) vector produces the chemokine with no fusion partner and leaves only an N-terminal Met and a C-terminal His tag of 8 amino acids. For the pET32LIC expression of MIP(7), the enterokinase cleavage appeared to result in several extra amino acids at the N-terminus of the protein, as evidenced by SDS−polyacrylamide gel electrophoresis and the appearance of several extra peaks in the NMR spectra of the protein. Protein samples were lyophilized and for NMR samples the protein was dissolved in 20 mM sodium phosphate, pH 2.5, with or without 150 mM NaCl. All NMR samples were made to 5% D_2O (Isotec).

NMR Spectroscopy. All spectra were recorded at 25 °C on a Varian UnityPlus 600 MHz spectrometer, equipped with a *z*-shielded gradient triple-resonance probe. Sample tubes were from Shigemi Inc. (Allison Park, PA). HSQC spectra were acquired with 512* points in the ^1H (direct) dimension and 64* points in the nitrogen dimension, where *n** represents *n* complex points. Spectral width for ^1H was 8000 Hz and for ^{15}N was 1700.68 Hz. Total acquisition times were 64 ms for the ^1H and 37.6 ms for the ^{15}N dimension. After processing, final hertz per point resolution was 5.2 for ^1H and 8.9 for ^{15}N. Referencing is relative to DSS, by the method proposed by Wishart et al. (*36*).

Relaxation Measurements. ^{15}N T_1, T_2, and $^{15}N\{-H\}$ *NOE* values were determined for 0.69 mM MIP-1β and 0.43 mM MIP(9) from two-dimensional spectra collected with pulse sequences described previously by Tjandra et al. (*37*) and Farrow et al. (*38*). The ^{15}N T_1 data were collected with ^{15}N delays of 21, 61, 121, 251, 361, 521, 761, 1001, and 1251 ms. The ^{15}N T_2 data were collected with ^{15}N delays of 16, 32, 48, 80, 96, 112, 144, and 160 ms. An additional time point with a delay of 192 ms was acquired for the MIP(9) sample. A delay of 1 s was used between scans. A $^{15}N-\{^1H\}$ *NOE* data set consists of two 2D spectra, one collected with ^1H saturation and one collected without. The delay between scans was 5 s and the presaturation period was 3 s. The two spectra were collected in an interleaved fashion. Likewise, all T_1 and T_2 data were collected in an interleaved fashion so that spectrometer drift effects were minimized. That is, at each t_1 increment, data for each of the eight or nine delays were collected. Furthermore, for MIP-1β, two data sets of 32 scans each were collected for T_1 and T_2, several days apart and using a different randomized order of delays. Only one T_1 and one T_2 data sets were acquired for MIP(9). Two 24-scan and one 48-scan *NOE* data sets were collected for wild-type MIP-1β and MIP(9), respectively. The total time used for data collection was 34.2 h for each 32-scan T_1 data set, 28.5 and 32.4 h for the T_2 data sets for MIP-1β and MIP(9), and 25.5 and 41.5 h for the *NOE* data sets for MIP-1β (0.69 mM) and MIP(9) (0.43 mM), respectively. All data sets were collected in the 2D mode, with the ^1H carrier set at the H_2O frequency and the ^{15}N carrier positioned at 118.1 ppm. Each 2D spectrum was collected as a 160* × 512* matrix, with acquisition times of 94 (t_1) and 64 ms (t_2).

All T_1, T_2, and *NOE* data sets were processed with 90°-shifted sine-bell apodization in t_1, truncated at sin (176°), and squared sine-bell apodization in t_2, truncated at $\sin^2$ (176°). The data were then zero-filled to a final digital resolution of 3.3 (F_1) and 5.2 Hz (F_2). The data were processed with the program nmrPipe (*39*), and 2D peak positions were determined with the program PIPP (*40*). Peak intensities were determined with the programs PIPP and seriesTab (F. Delaglio, unpublished results). T_1 and T_2 values were determined by fitting the measured 2D peak intensities as a function of the ^{15}N delay to a two-parameter single-exponential decay function, $I(t) = I_0 \exp(-t/T_{1,2})$, by nonlinear least-squares optimization with the program modelXY (F. Delaglio, unpublished results).

RESULTS AND DISCUSSION

To study the effects of N-terminal modification on the CC chemokine MIP-1β, we have pursued a strategy that combines mutagenesis with structural analysis using relatively quick nuclear magnetic resonance (NMR) experiments. The 2D HSQC spectrum (shown for wild-type MIP-1β in Figure 2A) gives a peak for each directly bonded NH pair in a protein, and the position of each peak is quite sensitive to changes in the environment of those nuclei. This type of spectrum is useful in providing immediate evidence regarding the foldedness of a protein, as the peaks in an unfolded protein resonate in a narrow region centered around 8.2 ppm

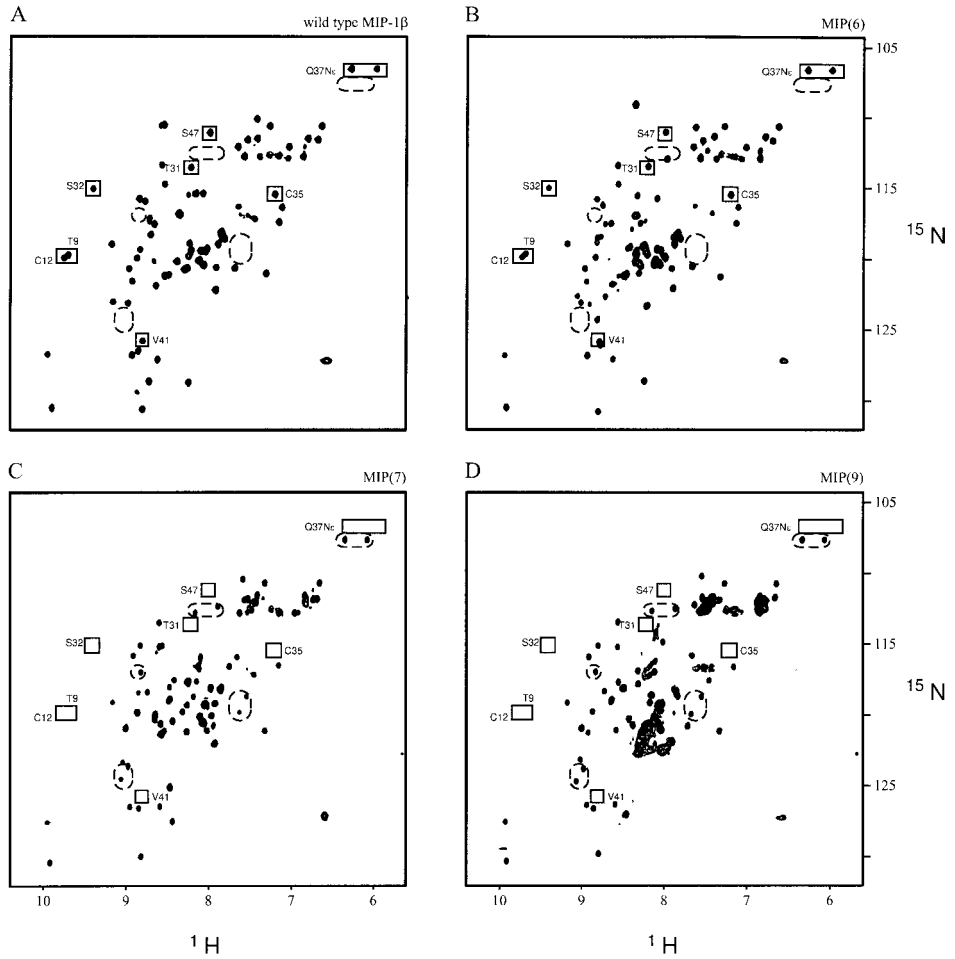

FIGURE 2: Two-dimensional HSQC NMR spectra of (A) 0.69 mM wild-type MIP-1β, (B) 0.70 mM MIP(6), (C) 0.75 mM MIP(7), and (D) 0.43 mM MIP(9) in 20 mM sodium phosphate. Solid rectangular boxes enclose peaks that correspond to residues important to dimerization. Dashed ovals indicate the placement of new peaks presumed to represent the protein in its monomeric form.

in the ^{1}H dimension (*41*, *42*). Each protein has a unique, identifiable spectrum and the HSQC spectrum provides insight about the environment of each backbone NH of a protein. MIP-1β forms ordered aggregates above pH 3.5, which may play a role in its function (*3*), so the spectra presented here were uniformly measured at pH 2.5. While this pH is unusually low, the CC chemokine subfamily shares the pH sensitivity, and most CC chemokine spectra are recorded well below neutral values (*6*, *9*). However, the structures of the CC chemokine dimers are remarkably consistent with each other, including those amenable to higher pH values such as MCP-1, the structure of which was determined at pH 5.4 (*10*).

Figure 2A shows the HSQC spectrum for wild-type MIP-1β, a 69 residue protein that one of us has previously shown to be a homodimer (*3*). As the structure of this protein has previously been determined, each NH resonance in the spectrum is assigned to a particular residue, and assignments important for our present discussion are shown in the figure. Several backbone amides in the dimer interface resonate at high frequency, facilitating identification, particularly those of Thr9 and Cys12, both of which appear above 9.5 ppm. The NH_2 side chain of Gln37 is also an important structural indicator, making contact with Cys11, Cys12, and Phe13 of its own subunit. These three amino acids are part of the dimer interface, so the chemical shift of the Gln37 side chain is expected to be sensitive to the presence or absence of the chemokine dimer. In addition, Ser32 is also an indirect indicator of the dimer, as it has several short contacts with the key dimer residue Thr9.

N-Terminal Truncation Mutants. We first truncated wild-type MIP-1β by removing the first five amino acids. To maintain a consistent naming convention, this protein that begins with amino acid Asp6 will be referred to as MIP(6). The 2D HSQC spectrum for MIP(6) is shown in Figure 2B. While it is missing the resonances for amino acids 1−5, the spectrum for MIP(6) is quite similar to that for the wild-type protein, particularly in the regions where dimer interface peaks resonate. This overall similarity leads us to conclude that even though five N-terminal residues have been removed from the wild-type protein, the structure of MIP(6) does not vary greatly from that of the wild-type MIP-1β, and the dimer interface of the protein is intact.

The MIP(7) mutant is missing the first 6 amino acids from wild-type MIP-1β, and begins with Pro7. Figure 2C shows interesting changes in the HSQC spectrum of this protein relative to those of the wild type and the MIP(6) mutant. Most importantly, the peaks from amino acids at the dimer interface have moved significantly or disappeared from their previous positions, particularly those from amino acids Thr9 and Cys12. Additionally, significant change has occurred for amino acids that interact with dimer interface residues, such as Ser32 and the side chain of Gln37. This shift in peak position for dimer residues indicates that these amino

acids are in a different environment in MIP(7) than in the wild-type protein. Also notable are new peaks in the spectrum, indicated by dashed ovals in Figure 2C. This spectrum suggests the presence of a new structural form of MIP-1β for this mutant. Given the wide chemical shift dispersion of the spectrum, the new form of the protein is evidently folded, and because this mutant contains significant N-terminal truncation, we hypothesize that this new form of the protein is monomeric MIP-1β. A small amount of the dimeric form of the protein also exists in solution, as evidenced by the presence of peaks arising from amino acids at or near the dimer interface when the spectrum is viewed at very low contour level (data not shown).

This original MIP(7) was expressed containing an uncleavable eight amino acid C-terminal His tag, which should be far removed from the site of dimerization (see Figure 1). However, the other proteins we report have been expressed to contain no C-terminal tail, so to control for possible differences between the two expression systems, we produced MIP(7) in the same vector (pET32LIC) as used for the wild-type and other mutant proteins reported here. In this case we found that cleaving the fusion partner to produce unmodified MIP(7) resulted in the probable existence of a few extra amino acids at the N-terminus of the protein, as judged by polyacrylamide gel electrophoresis and extra peaks in the unfolded region (around 8.2 ppm) of the HSQC spectrum (data not shown). However, each of the new (presumably monomer) peaks observed for the original MIP-(7) (Figure 2C) clearly appears on the spectra from the control MIP(7). Furthermore, while the control MIP(7) produced from pET32LIC (data not shown) has a higher proportion of dimer than the original MIP(7) mutant, the overall trends reported below are identical for each MIP(7).

To further mutate MIP-1β, we removed the first 8 amino acids to form MIP(9), a protein that begins with Thr9. The spectrum of this protein (Figure 2D) again reveals one folded species in solution, quite similar to that seen for MIP(7). No dimer interface peaks are identifiable in the MIP(9) spectrum, indicating that the amino acids around the dimer interface of the wild-type protein are in a different environment in this mutant. The new peaks from the MIP(7) spectrum are clearly evident in the MIP(9) spectrum, as shown by the dotted circles in Figure 2D. In the MIP(9) mutant, at least five amino acids that make dimer contacts in the wild-type protein have been removed, and so the very different spectrum seen for this protein in comparison to that for the wild-type protein indicates that MIP(9) is a monomeric variant of MIP-1β. In addition, while the MIP(7) and MIP(9) spectra are not identical, they are quite similar in most regions of the spectra, indicative of similar structural forms of MIP-1β. The presence of apparently unresolved peaks at approximately 8.0−8.2 ppm suggests that portions of the structure of MIP(9) may be less well defined than the wild type despite maintaining the overall integrity of the fold.

To investigate whether the new form of MIP-1β caused by N-terminal truncation is in fact a monomer, we measured spectra of dilute protein. Figure 3A shows the HSQC spectrum of wild-type MIP-1β diluted to 100 μM in 20 mM phosphate buffer. At low contour levels, new peaks are visible in this spectrum, in similar chemical shift positions as those seen for the N-terminal deletion mutants. This concentration dependence is expected for a monomer−dimer equilibrium and indicates that the new peaks do indeed correspond to a monomeric MIP-1β. Similarly, dilution of the MIP(6) mutant resulted in these new peaks on the HSQC spectrum (data not shown), indicating that at lower concentrations MIP(6) also begins to dissociate to the monomeric form. As a control, we diluted the MIP(7) variant and, as expected, saw no change of peak position at 100 μM protein concentration under low salt conditions (data not shown). Furthermore, dilution of MIP(9) resulted in no change in the HSQC spectra (data not shown), indicating that this extensively truncated protein is already purely monomeric at both high and low concentrations.

Determination of Rotational Correlation Time. To confirm that the HSQC peaks that arise upon N-terminal truncation and upon dilution belong to the MIP-1β monomer, we performed ^{15}N relaxation studies on wild-type MIP-1β and on the MIP(9) mutant in an effort to compare their relative rates of rotational diffusion. ^{15}N T_1, T_2, and *NOE* values were measured by established experimental methods (*37*, *38*, *43*, *44*). Two ^{15}N T_1, T_2, and *NOE* data sets were collected several days apart for wild-type MIP-1β and the pairwise root-mean-square-difference (rmsd) were 2.6%, 4.4%, and 11.4% of the average T_1, T_2, and *NOE* values, respectively. Therefore, the uncertainty in the average value is 1.3% for T_1, 2.2% for the T_2 and 5.7% for *NOE*. The uncertainty in the average T_1 and T_2 values as determined from the uncertainty in the nonlinear least-squares fitting of the decay curves were 3% and 2.7%, respectively. The rms noise indicates that the uncertainty in the averaged *NOE* is 4%. The uncertainties in the T_1 and T_2 values for MIP(9) as determined from the nonlinear least-squares fitting are 8.5% and 8.3%, respectively. The signal-to-noise ratios of the MIP(9) *NOE* spectra were about 3 times lower than for MIP-1β, and the uncertainty in the MIP(9) *NOE* values is estimated to be about 12.4%.

It is often assumed that the ^{15}N T_1/T_2 ratio provides a good measure of the global correlation time, τ_c (*43*), provided precautions are taken to exclude residues that experience either (1) internal motion slower than a few hundred picoseconds or (2) conformational exchange occurring on a microsecond to millisecond time scale. Residues that execute motions on a time scale slower than approximately 100 ps can be identified by their low *NOE* values. Therefore, residues with a ^{15}N{$^{-1}$H} *NOE* value less than 0.6 were excluded from further analysis. The following criterion can be used to identify residues experiencing slow conformational exchange (*37*, *44*):

$$(\langle T_2\rangle - T_{2,n})/\langle T_2\rangle - (\langle T_1\rangle - T_{1,n})/\langle T_1\rangle > 1.5\mathrm{SD} \quad (1)$$

$\langle T_2\rangle$ and $\langle T_1\rangle$ are the average T_2 and T_1 values, respectively, $T_{2,n}$ and $T_{1,n}$ are the T_2 and T_1 values of residue n, and SD is the standard deviation of $(\langle T_2\rangle - T_{2,n})/\langle T_2\rangle - (\langle T_1\rangle - T_{1,n})/\langle T_1\rangle$, excluding residues with a ^{15}N *NOE* < 0.6. Of the 69 residues of wild-type MIP-1β, six are prolines and are not observable in the ^{15}N/^{1}H^{N} spectra. Out of the remaining 63 residues, 59 peaks could be clearly assigned, and four were degenerate and not considered further. An additional 11 residues were eliminated on the basis of *NOE* values < 0.6 and another six were eliminated because of slow conformational exchange as defined by eq 1. Therefore, a total of 42 residues of wild-type MIP-1β were used in further calcula-

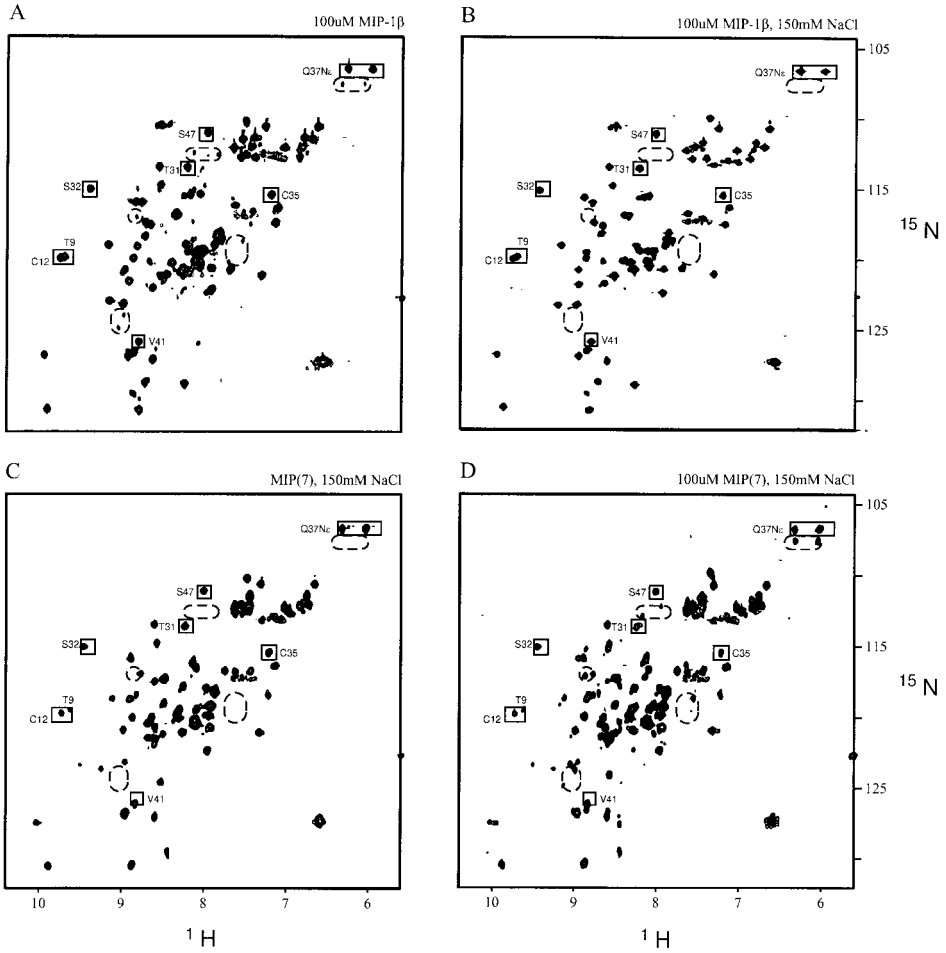

FIGURE 3: (A, B) Comparison of the two-dimensional HSQC NMR spectra of 100 μM wild-type MIP-1β at 20 mM sodium phosphate in the (A) absence and (B) presence of 150 mM NaCl. Spectra are displayed at low contour levels to show the presence of peaks indicative of monomeric protein under conditions of low ionic strength and the absence of these monomer peaks with the addition of physiological concentrations of salt. (C, D) HSQC experiments performed on the N-terminally truncated MIP-1β analogue MIP(7) at (C) 0.75 mM and (D) 100 μM concentrations. Both samples were made to 20 mM sodium phosphate and 150 mM NaCl. Solid boxes highlight important peaks known to correspond to the dimer, whereas dashed ovals point out the position of peaks belonging to the monomeric species.

tions. The average ^{15}N relaxation times for the 42 residues are $T_1 = 708 \pm 51$ ms and $T_2 = 85 \pm 5$ ms. MIP(9) has 58 nonproline residues of which 50 (unassigned) correlations were picked in the 2D spectra. Eighteen residues displayed *NOE* values less than 0.6 and were excluded from further analysis. Of the remaining 32, five were eliminated by use of eq 1. A total of 27 residues of MIP(9) were used in further calculations. The average ^{15}N relaxation times for the 27 residues are $T_1 = 424 \pm 47$ ms and $T_2 = 136 \pm 14$ ms. The average ^{15}N T_1/T_2 ratios for wild-type MIP-1β and MIP(9) are 8.3 ± 0.8 and 3.1 ± 0.3, respectively.

Shown in Figure 4 is a histogram of the 48 and 32 ^{15}N T_1/T_2 ratios of wild-type MIP-1β and MIP(9), where the corresponding *NOE* $\geq$ 0.6. Equations for ^{15}N T_1, T_2, and ^{15}N{$^{-1}$H} *NOE* as a function of τ_c are given elsewhere (*37*, *38*, *43*, *44*). After elimination of residues experiencing slow conformational exchange (eq 1), the isotropic rotational correlation time, τ_c, was found by minimizing:

$$E = \sum_n [(T_1^{obs}/T_2^{obs}) - (T_1^{pred}/T_2^{pred})]^2/\Delta^2 \qquad (2)$$

T_1^{obs} and T_2^{obs} are the experimentally determined ^{15}N relaxation times, T_1^{pred} and T_2^{pred} are the calculated ^{15}N relaxation times, assuming isotropic tumbling, Δ is the estimated uncertainty in the T_1^{obs}/T_2^{obs} ratio, and n goes from 1 to N, where N is the number of residues used in the summation. The uncertainty in τ_c was estimated by repeatedly deleting 20% of the experimental ratios, selected randomly, and then determining τ_c from the remaining 80%. After 200 such cycles of random deletion followed by E

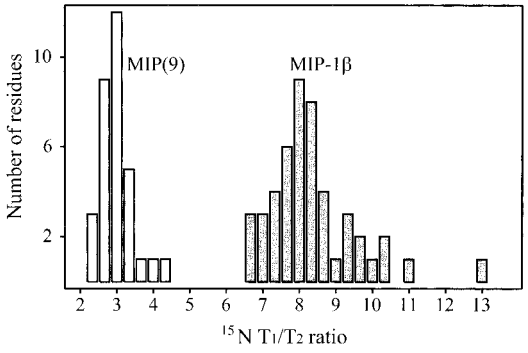

FIGURE 4: Histogram showing the number of amino acids possessing various ^{15}N T_1/T_2 ratios and *NOE* values $\geq$ 0.6. A shaded bar is used to represent the population of T_1/T_2 ratios for MIP-1β within $\pm$0.33 width, while a white bar is used to represent the population of T_1/T_2 ratios for MIP(9). A total of 48 and 32 experimental ratios were used to create the histograms for MIP-1β and MIP(9), respectively. The average T_1/T_2 ratios for MIP-1β and MIP(9) shown in these histograms are 8.5 ± 1.2 and 3.2 ± 0.4, respectively.

minimization, the average τ_c was 8.6 ± 0.1 ns for wild-type MIP-1β (*E/N* = 11) and 4.5 ± 0.1 ns for MIP(9) (*E/N* = 1).

These relaxation data strongly indicate that wild-type MIP-1β, at millimolar concentrations, exists as a dimer and that MIP(9) exists as a monomer. As the data are collected from largely resolved two-dimensional spectra, τ_c values could be correlated with peaks in the MIP-1β and MIP(9) spectra. Given the chemical shift similarities between MIP(9) and MIP(7), the data suggest that MIP(7) also exists predominantly in the monomeric form under the conditions described for Figure 2C. It is important to note that the reported rotational correlation times for wild-type MIP-1β and MIP-(9) were determined under the assumption that the molecules execute isotropic tumbling. The NMR-derived structure of MIP-1β is not well described by a sphere and should tumble anisotropically, as is evident from the principal components of its inertia tensor, relative to its center of mass, 1:0.97:0.25, and from the relatively high *E/N* value of 11. The relative ratios of the principal components of the inertia tensor for MIP(9) are estimated to be 1:0.91:0.63. A full anisotropic treatment of the data for both MIP-1β and MIP-(9) (which has not yet been fully assigned) is outside the scope of this report and will be presented elsewhere.

Solution Conditions Affect Oligomeric State. The N-terminal dimer interface of MIP-1β has significant hydrophobic character, and the dimerization of this protein results in significant burial of hydrophobic surfaces (*3*). Therefore, we reasoned that dimer−monomer equilibrium may be sensitive to the salt concentration of the sample and that this dependence may be relevant to the current debate regarding the presence of dimer at physiological concentrations. The results we report above were carried out at low salt concentrations (20 mM sodium phosphate), but the concentration of salt in the blood is much higher, being 142 mM sodium and 104 mM chloride (*45*). Others have reported that solution conditions affect the oligomeric state of the chemokine (*6*), with higher ionic strength favoring the tetramer over the dimer and monomer for PF-4 (*46*), while high ionic strength weakens dimer affinity for IL-8 (*22*). Therefore, we measured spectra of wild-type and mutant MIP-1β under various conditions to determine the dependence of physiological salt concentrations on the dimer−monomer equilibrium.

Figure 3 shows the effect of salt on wild-type and mutant MIP-1β. While Figure 3A shows 100 μM MIP-1β in the presence of only 20 mM sodium phosphate, Figure 3B shows the same concentration of protein in the presence of both 20 mM sodium phosphate and 150 mM NaCl. The peaks that had been assigned to trace amounts of monomeric protein are completely gone in the high-salt sample (as shown by the dotted ovals in Figure 3B), and only dimer peaks remain. A similar effect is seen for the mutant MIP(6) at 100 μM protein, as the presence of 150 mM NaCl results in a spectrum devoid of any monomer peaks (data not shown).

We extended our examination of salt effects to the MIP-1β mutant MIP(7). We have already established that under low salt conditions this N-terminal truncation mutant that begins at Pro7 is largely monomeric. Figure 2C shows the HSQC spectrum of 0.75 mM MIP(7) with 20 mM phosphate, while Figure 3C shows the same concentration of protein with additional 150 mM NaCl. We see a clear change in the spectrum, with the reappearance of peaks indicative of the MIP-1β dimer (solid boxes) and an obvious diminution of peaks corresponding to the monomeric form (dashed ovals). The experiment on MIP(7) was then repeated at a lower (100 μM) protein concentration. Under low salt conditions, this dilute MIP(7), as expected, yielded spectra indicative of fully monomeric protein (data not shown). However, upon addition of 150 mM NaCl, the spectrum indicates a mixture of monomer and dimer, as shown in Figure 3D. In both spectra of MIP(7) that were measured under high salt conditions, new peaks appear above 9 ppm that are not observed in spectra of the other mutants. These peaks are likely associated with the dimeric form of MIP(7) and result from adjustments at the interface induced by removal of several N-terminal amino acids compared to the wild type. We have also begun a preliminary examination of the mutant MIP(8), which begins with Pro8. We have found that this mutant is a monomer under low salt conditions and that the presence of 150 mM NaCl again results in the appearance of dimer peaks in the HSQC spectrum (unpublished results).

Chemokine	N-terminus	β0	N-loop
MIP-1β	APMGSDPP	TAC	CFSYTARKLP...
MCP-1	QPDAINAP	VTC	CYNFTNRKIS...
RANTES	-SPYSSDT	TPC	CFAYIARPLP...

FIGURE 5: Sequence alignment of the N terminus of three CC chemokines that form similar dimeric structures. The N-loop region is composed of the amino acids that form a loop between the interfacial β strand (β0) and the first strand of the core domain.

To investigate the effect of salt on the mutant MIP(9), a 0.8 mM protein sample was made to 150 mM NaCl (data not shown). These conditions led to the gradual precipitation of the protein, and on the HSQC spectrum no peaks were observed that could be assigned to the dimeric protein. Apparently, while the MIP(9) variant is a stable, folded monomer under low salt conditions, it cannot be forced into a dimer and the presence of salt destabilizes the protein at high concentrations.

The presence of physiological salt concentrations clearly has a powerful effect on the dimer−monomer equilibrium for MIP-1β, strongly favoring the chemokine dimer. This effect is seen for the wild-type protein and for each variant except for MIP(9), which apparently has lost the ability to dimerize. While the protein concentrations reported here are higher than those used in biological assays, our preliminary NMR data show no evidence of a MIP-1β monomer at 10 μM protein concentration and 150 mM NaCl (unpublished results). Our present work, in conjunction with the recent report demonstrating the ability of cell surface sugars to locally concentrate chemokines (*27*), indicates that the MIP-1β dimer may be a physiologically relevant species. In addition, we suggest that functional changes in other N-terminally truncated chemokines may be due in part to their relative inability to dimerize.

While sequence alignment of MIP-1β with the CC chemokines MCP-1 and RANTES (Figure 5) shows that there is significant deviation between amino acid composition of the N-terminal region, a structural comparison reveals conservation of the overall fold, including the area that comprises the dimer interface (*3*, *6*, *9*, *10*). For each protein there is an intersubunit antiparallel β-strand interaction around residues 9−11 (MIP-1β numbering) and there are

intermolecular contacts made by the preceding several amino acids that stabilize the chemokine homodimer. On the basis of the overall fold and local structural similarities between these three CC chemokines, we believe that the changes in dimer stability of MIP-1β upon N-terminal truncation are representative of the effects of N-terminal truncation for MCP-1 and RANTES. For example, Asp6 in MIP-1β interacts across the dimer with Thr16, Gln49, Val50, and Cys51. The MIP(6) mutant (which has lost the first five amino acids but does retain Asp6) shows no change in any of the peaks corresponding to these four residues (peaks not identified in Figure 2B). However, the spectra for MIP(7) and MIP(9) reveal that at least Thr16 and Val50 (the two most easily identifiable of the four residues) have changed environment, as evidenced by such significant shifts in peak position that they no longer can be identified. In addition, a host of new peaks arise in the spectra for MIP(7) and MIP-(9), indicating the presence of a protein monomer (Figure 2C,D).

Our results indicate that Asp6 is quite important in allowing MIP-1β dimer formation, and this conclusion may be relevant to functional studies involving MCP-1. The analogous residue in MCP-1 is Asn6, which makes comparable contacts (to Thr16, Ile51, and Cys52) across its dimer interface. In relevant functional work, Gong and Clark-Lewis assayed a series of truncated MCP-1 mutants for their ability to induce chemotaxis and mobilize calcium. The data reveal that removal of residues up to Asn6 permits the chemokine to retain partial functionality, although the activity of mutants starting with residues 2, 3, and 4 are notably reduced (*29*). Truncation of Asn6 (and any further truncation) led to proteins that act as potent antagonists with regard to the wild-type protein. Considering the number of close contacts made by the residue at that position, it seems likely that this truncation greatly reduces the dimer affinity of the protein and this may in part lead to the striking functional difference caused by the truncation. In addition, the large variations in activity observed for variants that still possess Asn6 illustrate the complexity of action of chemokines, wherein some amino acids of the N-terminus are crucial for activity but probably not for dimerization (such as amino acids 2−4), and some are clearly necessary for dimerization and may also affect activity (such as amino acid 6). We do not yet know whether receptor activation requires a CC chemokine dimer, but several truncated variants of MCP-1 are likely to be monomeric, and these antagonize but do not exhibit MCP-1 activity (*29*). These results are consistent with a chemokine dimer being important for activity.

Several N-terminal mutants have also been reported for the CC chemokine RANTES, which can also be cautiously interpreted from a structural standpoint. Ser5 of RANTES is structurally analogous to Asp6 of MIP-1β, which we have found to be important in stabilizing the chemokine dimer. While results for any truncation mutant that retains residue 5 have not been reported, it has been shown that RANTES variants beginning with residue 6, 7, 8, 9, or 10 are all antagonists of RANTES action. In addition, RANTES(9−68) (which lacks the first eight amino acids of the protein) not only is an antagonist for wild-type RANTES activity, but has gained specificity for other chemokine receptors (*31*). On the basis of our observations for MIP-1β, it is likely that this truncation mutant of RANTES has little potential for dimerization, and the less truncated variants also have greatly weakened dimer affinities. This leads again to the possibility that although a chemokine monomer can bind at the cell surface, the details of dimer formation impart some amount of specificity and activity to the protein. The importance of gaining a greater understanding of the structural reasons for the binding and activity of truncated chemokines is illustrated by the observation that, despite lacking activity, RANTES-(9−68) retains the ability to bind to the receptor CCR5 and as such possesses potent anti-HIV activity (*34*).

In other work on RANTES, alanine scanning mutagenesis was used to identify individual amino acids at or near the N-terminus of the protein that are important for receptor binding or activation (*33*). These workers support a "two-site" model of receptor binding wherein amino acids near the N-terminus are necessary for receptor activation, while amino acids at position 10−20 comprise another site that, if intact, allows tight binding. Aside from amino acids 2 and 3, each identified crucial site in RANTES (Asp6, Thr7, Phe12, Ile15, and Arg17) is analogous to an important dimer interface residue in MIP-1β (*33*). Therefore, it is likely that a mutation at any of these sites would diminish the ability of the mutant to dimerize.

CONCLUSION

We have used NMR to show the structural effects of N-terminal truncation on the CC chemokine MIP-1β. This protein, along with some others in the CC family, has been shown to block HIV infection (*14*−*16*), but the oligomeric state of the chemokines as they carry out this and other important functions remains controversial. We show that while the protein maintains a dimeric structure upon the removal of its first five amino acids, the dimer is considerably weakened with the loss of Asp6, and the ability to dimerize appears to be abolished upon removal of the first eight amino acids. The presence of physiological (150 mM) sodium chloride dramatically increases dimer affinity in MIP-1β, suggesting the presence of chemokine dimers at micromolar or lower protein concentrations. This work represents an investigation of the elements involved in chemokine dimer affinity and provides a structural framework for interpretation of a wide range of functionally important chemokine mutants.

ACKNOWLEDGMENT

We gratefully acknowledge Rica Bruinsma and Kristina Lain for assistance with protein preparation and Frank Delaglio for technical assistance with nmrPipe. We are also thankful to Dean Carlson for technical assistance.

REFERENCES

1. Oppenheim, J., J., Zachariae, C. O. C., Mukaida, N., and Matsushima, K. (1991) *Annu. Rev. Immunol. 9*, 617−648.
2. Schall, T. J. (1991) *Cytokine 3*, 165−183.
3. Lodi, P. J., Garrett, D. S., Kuszewski, J., Tsang, M. L.-S., Weatherbee, J. A., Leonard, W. J., Gronenborn, A. M., and Clore, G. M. (1994) *Science 263*, 1762−1767.
4. Clore, G. M., Appella, E., Yamada, M., Matsushima, K., and Gronenborn, A. M. (1990) *Biochemistry 29*, 1689−1696.
5. Zhang, X., Chen, L., Bancroft, D. P., Lai, C. K., and Maione, T. E. (1994) *Biochemistry 33*, 8361−8366.
6. Skelton, N. J., Aspiras, F., Ogez, J., and Schall, T. J. (1995) *Biochemistry 34*, 5329−5342.

7. Kim, K.-S., Rajarathnam, K., Clark-Lewis, I., and Sykes, B. D. (1996) *FEBS Lett. 395*, 277−282.
8. Meunier, A., Bernassau, J.-M., Guillemot, J.-C., Ferrara, P., and Darbon, H. (1997) *Biochemistry 36*, 4412−4422.
9. Chung, C., Cooke, R. M., Proudfoot, A. E. I., and Wells, T. N. C. (1995) *Biochemistry 34*, 3907−9314.
10. Handel, T. M., and Domaille, P. J. (1996) *Biochemistry 35*, 6569−6584.
11. Fairbrother, W. J., Reilly, D., Colby, T. J., Hesselgesser, J., and Horuk, R. (1994) *J. Mol. Biol. 242*, 252−270.
12. Lubkowski, J., Bujacz, G., Boque, L., Domaille, P. J., Handel, T. M., and Wlodawer, A. (1997) *Nat. Struct. Biol. 4*, 64−69.
13. Crump, M. P., Gong, J.-H., Loetscher, P., Rajarathnam, K., Amara, A., Arenzana-Seisdedos, F., Virelizier, J. L., Baggiolini, M., Sykes, B. D., and Clark-Lewis, I. (1997) *EMBO J. 16*, 6996−7007.
14. Deng, H., Liu, R., Ellmeier, W., Choe, S., Unutmaz, D., Burkart, M., DiMarzio, P., Marmon, S., Sutton, R. E., Hill, C. M., Davis, C. B., Peiper, S. C., Schall, T. J., Littman, D. R., and Landau, N. R. (1996) *Nature 381*, 661.
15. Alkhatib, G., Combadiere, C., Broder, C. C., Feng, Y., Kennedy, P. E., Murphy, P. M., and Berger, E. A. (1996) *Science 272*, 1955−1958.
16. Drajic, T., Litwin, V., Allaway, G. P., Martin, S. R., Huang, Y., Nagashima, K. A., Cayanan, C., Maddon, P. J., Koup, R. A., Moore, J. P., and Paxton, W. A. (1996) *Nature 381*, 667−673.
17. Samson, M., Labbe, O., Mollereau, C., Vassart, G., and Parmentier, M. (1996) *J. Biol. Chem. 35*, 3362−3367.
18. Rajarathnam, K., Sykes, B. D., Kay, C. M., Dewald, B., Geiser, T., Baggiolini, M., and Clark-Lewis, I. (1994) *Science 264*, 90−92.
19. Burrows, S. D., Doyle, M. L., Murphy, K. P., Franklin, S. G., White, J. R., Brooks, I., McNulty, D. E., Scott, M. O., Knutson, J. R., Porter, D., Young, P. R., and Hensley, P. (1994) *Biochemistry 33*, 12741−12745.
20. Paolini, J. F., Willard, D., Consler, T., Luther, M., and Krangel, M. S. (1994) *J. Immunol. 153*, 2704−2717.
21. Mantel, C., Kim, Y. J., Cooper, S., Kwon, B., and Broxmeyer, H. E. (1993) *Proc. Natl. Acad. Sci. U.S.A. 90*, 2232−2236.
22. Lowman, H. B., Fairbrother, W. J., Slagle, P. H., Kabakoff, R., Liu, J., Shire, S., and Hébert, C. A. (1997) *Protein Sci. 6*, 598−608.
23. Leong, S. R., Lowman, H. B., Liu, J., Shire, S., Deforge, L. E., Gillece-Castro, B. L., McDowell, R., and Hébert, C. A. (1997) *Protein Sci. 6*, 609−617.
24. Tanaka, Y., Adams, D. H., Hubscher, S., Hirano, H., Siebenlist, U., and Shaw, S. (1993) *Nature 361*, 79−82.
25. Koopmann, W., and Krangel, M. S. (1997) *J. Biol. Chem. 272*, 10103−10109.
26. Graham, G. J., MacKenzie, J., Lowe, S., Tsang, L.-S., Weatherbee, J. A., Issacson, A., Medicherla, J., Fang, F., Wilkinson, P. C., and Pragnell, I. B. (1994) *J. Biol. Chem. 269*, 4974−4978.
27. Hoogewerf, A. J., Kuschert, G. S. V., Proudfoot, A. E. I., Borlat, F., Clark-Lewis, I., Power, C. A., and Wells, T. N. C. (1997) *Biochemistry 36*, 13570−13578.
28. Zhang, Y., and Rollins, B. J. (1995) *Mol. Cell. Biol. 15*, 4851−4855.
29. Gong, J.-H., and Clark-Lewis, I. (1995) *J. Exp. Med. 181*, 631−640.
30. Clark-Lewis, I., Kim, K.-S., Rajarathnam, K., Gong, J.-H., Dewald, B., Moser, B., Baggiolini, M., and Sykes, B. D. (1995) *J. Leukocyte Biol. 57*, 703−711.
31. Gong, J.-H., Uguccioni, M., Dewald, B., Baggiolini, M., and Clark-Lewis, I. (1996) *J. Biol. Chem. 271*, 10521−10527.
32. Weber, M., Uguccioni, M, Baggiolini, M., Clark-Lewis, I., and Dahinden, C. A. (1996) *J. Exp. Med. 183*, 681−685.
33. Pakanathian, D. R., Kuta, E. G., Artis, D. R., Skelton, N. J., and Hébert, C. A. (1997) *Biochemistry 36*, 9642−9648.
34. Arenzana-Seisdedos, F., Virelizier, J.-L., Rousset, D., Clark-Lewis, I., Loetscher, P., Moser, B., and Baggiolini, M. (1996) *Nature 383*, 400.
35. van Kimmenade, B., M. W., Schumacher, J. H., Laquoi, C., and Kastelein, R. A. (1988) *Eur. J. Biochem. 173*, 109−114.
36. Wishart, D. S., Bigam, C. G., Yao, J., Abildgaard, F., Dyson, H. J., Oldfield, E., Markley, J. L., and Sykes, B. D. (1995) *J. Biomol. NMR 6*, 135−140.
37. Tjandra, N., Feller, S. E., Pastor, R. W., and Bax, A. (1995) *J. Am. Chem. Soc. 117*, 12562−12566.
38. Farrow, N. A., Muhandiram, R., Singer, A. U., Pascal, S. M., Kay, C. M., Gish, G., Shoelson, S. E., Pawson, T., Forman-Kay, J. D., and Kay, L. E. (1994) *Biochemistry 33*, 5984−6003.
39. Delaglio, F., Grzesiek, S., Vuister, G. W., Zhu, G., Pfeifer, J., and Bax, A. (1995) *J. Biomol. NMR 6*, 277−293.
40. Garrett, D. S., Powers, R., Gronenborn, A. M., and Clore, G. M. (1991) *J. Magn. Reson. 95*, 214−220.
41. Frank, M. K., Clore., G. M., and Gronenborn, A. M. (1995) *Protein Sci. 4*, 2605−2615.
42. Huth, J. R., Bewley, C. A., Jackson, B. M., Hinnebusch, A. G., Clore, G. M., and Gronenborn, A. M. (1997) *Protein Sci. 6*, 2359−2364.
43. Kay, L. E., Torchia, D. A., and Bax, A. (1989) *Biochemistry 28*, 8972−8979.
44. Tjandra, N., Wingfield, P., Stahl, S., and Bax, A. (1996) *J. Biomol. NMR 8*, 273−284.
45. Rose, B. D. (1994) *Clinical Physiology of Acid−Base and Electolyte Disorders*, 4th ed., McGraw-Hill Inc., New York.
46. Mayo, K. H., and Chen, M.-J. (1989) *Biochemistry 28*, 9469−9478.

BI980329L